Supplemental Material

Full conflict-of-interest statement: RZ is an inventor on the following patents and patent applications: “Treatment Of Glycolysis-Low And Glycolysis-High Tumors With CTLA-4 Inhibitors” (US provisional application 63/310,089); “CD4+ TFH-Like Cells as a Therapeutic Target (international application PCT/US2021/055992); “Inhibition of CTLA-4 and/or PD-1 for Regulation of T cells” (US provisional patent 62/582,416); “Antibodies and Methods of Use Thereof” (US provisional patent application WO2018106864A1); “Anti-PD-1 Antibodies and Methods of Use Thereof” (US patent application US10323091B2); and “Anti-GITR Antibodies and Methods of Use Thereof” (patent application US20180244793A1). RZ is a scientific advisory board member of iTEOS Therapeutics and receives grant support from AstraZeneca and Bristol Myers Squibb. JDW is a consultant for Apricity; Ascentage Pharma; AstraZeneca; BeiGene; Bicara Therapeutics; Bristol Myers Squibb; Chugai, Daiichi Sankyo; Dragonfly; Imvaq; Larkspur; Psioxus, Recepta; Tizona; Trishula Therapeutics; and Sellas. JDW received grant/research support from Bristol Myers Squibb. JDW has equity in Apricity, Arsenal IO; Ascentage; CellCarta; Imvaq; Linneaus, Larkspur; Georgiamune; Maverick; Tizona Therapeutics; and Xenimmune. JDW is an inventor on the following patents: “Xenogeneic DNA Vaccines,” “Newcastle Disease Viruses for Cancer Therapy,” “Myeloid-Derived Suppressor Cell (MDSC) Assay,” “Prediction Of Responsiveness to Treatment With Immunomodulatory Therapeutics and Method of Monitoring Abscopal Effects During Such Treatment,” “Anti-PD1 Antibody”; “Anti-CTLA4 Antibodies,” and “Anti-GITR Antibodies and Methods of Use Thereof”. TM is a consultant for Immunos Therapeutics, Daiichi Sankyo Co., TigaTx, Normunity, and Pfizer; is a cofounder of and equity holder in IMVAQ Therapeutics; receives research funding from Bristol Myers Squibb, Surface Oncology, Kyn Therapeutics, Infinity Pharmaceuticals, Peregrine Pharmaceuticals, Adaptive Biotechnologies, Leap Therapeutics, and Aprea Therapeutics; and is a named inventor on patents listed in the table below.

Taha Merghoub Patents

https://patents.google.com/?inventor=Taha+Merghoub&oq=Taha+Merghoub+

Title:	Application number:	Filing Entity:
Antibodies and methods of use thereof	US11447557B2	Agenus Inc.
Replication competent attenuated vaccinia viruses with deletion of thymidine kinase with and without the expression of human Flt3L or GM-CSF for cancer immunotherapy	US11986503B2	Memorial Sloan Kettering Cancer Center
Anti-CTLA-4 antibodies and methods of use thereof	US11267889B2	Agenus Inc.
Methods of administering anti-OX40 antibodies	US11472883B2	Agenus Inc.
Anti-CTLA-4 antibodies and methods of use thereof	US11638755B2	Agenus Inc.
Anti-OX40 antibodies and anti-GITR antibodies	US11359028B2	Agenus Inc.
Anti-OX40 antibodies and methods of use thereof	US20210324097A1	Agenus Inc.

Anti-pd-1 antibodies and methods of use thereof	US20220372149A1	Agenus Inc.
Recombinant MVA or MVADELE3L expressing human FLT3L and use thereof as immuno-therapeutic agents against solid tumors	US12036279B2	Memorial Sloan Kettering Cancer Center
Neoantigens and uses thereof for treating cancer	EP3576781B1	Icahn School of Medicine at Mount Sinai
Use of inactivated nonreplicating modified vaccinia virus Ankara (MVA) as monoimmunotherapy or in combination with immune checkpoint blocking agents for solid tumors	US11426460B2	Memorial Sloan Kettering Cancer Center
Antibodies and method of use thereof	US20200024350A1	Agenus Inc.
Use of MVA or MVAΔE3L as immunotherapeutic agents against solid tumors	US11253560B2	Memorial Sloan Kettering Cancer Center
Anti-GITR antibodies and methods of use thereof	AU2022215304A1	Agenus Inc.
Anti-GITR antibodies and methods of use thereof	US20200123265A1	Agenus Inc.
Methods and compositions for tumor therapy	AU2016304597B2	Memorial Sloan Kettering Cancer Center
Anti-OX40 antibodies and method of use thereof	EP3383914A1	Agenus Inc.

Anti-GITR antibodies and methods of use thereof	WO2017096276A1	Agenus Inc.
Recombinant poxviruses for cancer immunotherapy	US20220056475A1	Memorial Sloan Kettering Cancer Center
BI-Specific activators for tumor therapy	US20240239910A1	Memorial Sloan Kettering Cancer Center
Alphavirus Replicon Particles Expressing TRP2	US20200113984A1	Alphavax, Inc.
Oncolytic Vaccinia virus expressing immune checkpoint blockade for cancer Immunotherapy	EP3765047A1	Memorial Sloan Kettering Cancer Center
Inducing favorable effects of tumor microenvironment via administration of nanoparticle compositions	EP3765047A1	Memorial Sloan Kettering Cancer Center
Vaccinia Virus mutants useful for cancer immunotherapy	US11884939B2	Memorial Sloan Kettering Cancer Center
Methods and compositions for treatment of pancreatic cancer	IL289251A	Memorial Sloan Kettering Cancer Center
Inhibition of CTLA-4 and/or PD-1 for Regulations of T Cells	US20210179714A1	Memorial Sloan Kettering Cancer Center
Heat-inactivated vaccinia virus as a vaccine immune adjuvant	EP3706768A1	Memorial Sloan Kettering Cancer Center
CD40 binding molecules and uses of thereof	CA3202384A1	Memorial Sloan Kettering Cancer Center
Antigen-binding proteins targeting melanoma differentiation antigens and uses thereof	US20190375855A1	Memorial Sloan Kettering Cancer Center

CD40 binding molecules and uses thereof	AU2021400733A9	Memorial Sloan Kettering Cancer Center
Anti-PD-1 antibodies and methods of use thereof	AU2021200281B2	Agenus Inc.
Anti-CTLA-4 antibodies and methods of use thereof	NZ794974A	Agenus Inc.
Peripheral blood phenotype linked to outcomes after immunotherapy treatment	US20240085417A1	Memorial Sloan Kettering Cancer Center
CD4+ TFH- like cells as a therapeutic target	US20230390390A1	Memorial Sloan Kettering Cancer Center
Antigen recognizing receptors targeting b7-h3 and uses there of	WO20224102685A2	Memorial Sloan Kettering Cancer Center
Anti-PD-1 Antibodies and their methods of use	AR105886A1	Agenus Inc.
Treatment of glycolysis-low and glycolysis-high tumors with CTLA-4 Inhibitors	WO2023154959A2	Memorial Sloan Kettering Cancer Center Office of Technology Development
II33 Proteints and methods of use thereof	WO2023081802A2	Memorial Sloan Kettering Cancer Center
Models for predicting mutant p53 fitness and their implications in cancer therapy	WO2022177989A1	Memorial Sloan Kettering Cancer Center
Chimeric receptor targeting muc16 and uses thereof	US20240189426A1	Memorial Sloan Kettering Cancer Center
Heteroclitic cancer vaccines	EP4121081A1	Memorial Sloan Kettering Cancer Center

Use of Composition, MVA?E3L and Pharmaceutically acceptable Vehicle of Diluent	BR112017022134B1	Memorial Sloan Kettering Cancer Center
Antibodies and Methods of its use	AR110348A1	Agenus Inc.
Phosphatidylserine targeting agents and uses thereof for adoptive t-cell	WO2019178207A1	Memorial Sloan Kettering Cancer Center
Recombinant poxviruses for cancer immunotherapy	WO2024097448A1	Memorial Sloan Kettering Cancer Center
Anti-CTLA-4 Antibodies and Methods of use of the same	AR104810A1	Agenus Inc.
Uso de composicao MVA?E3L e veiculo ou Diluente Farmaceuticamente aceitavel	BR112017022134B1	Memorial Sloan Kettering Cancer Center

Supplemental Figures

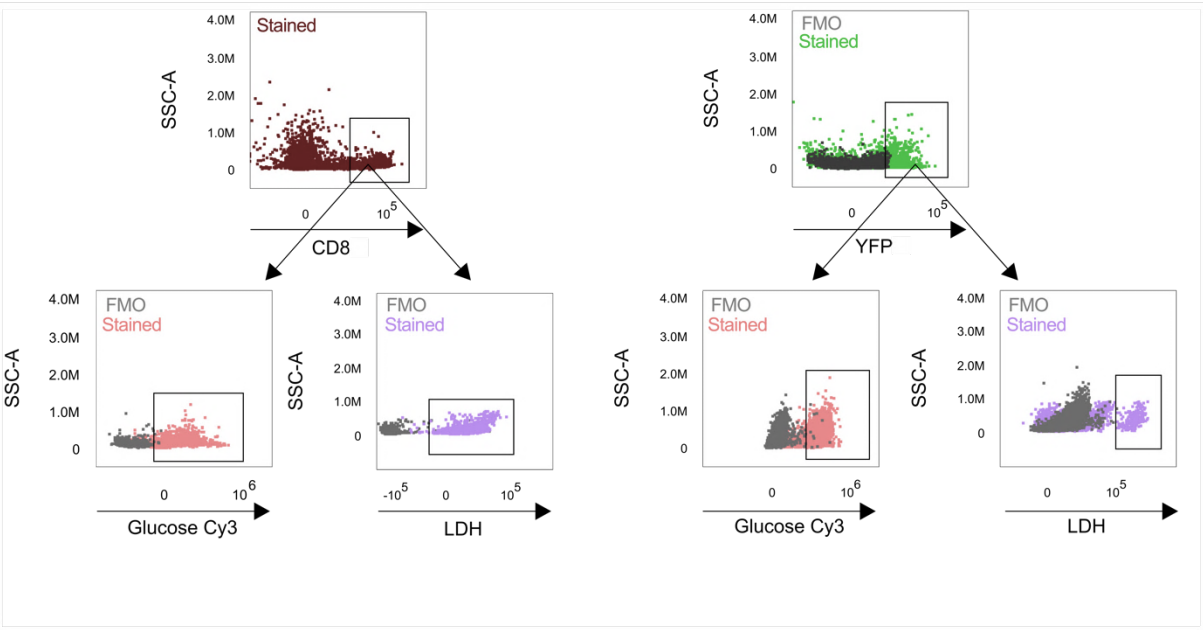

Supplemental Figure 1. Gating strategy for Glucose Cy3 and LDH in YFP$^+$ B16 tumor cells and CD8+ T cells. Flow cytometry dot plots for Glucose-Cy3 and intracellular LDH staining compared to unstained or isotype controls (FMO, gray) for tumor- infiltrating CD8+ T cells and YFP+ B16 tumor cells from established B16-YFP murine tumors (corresponding to Main Figure 1F).

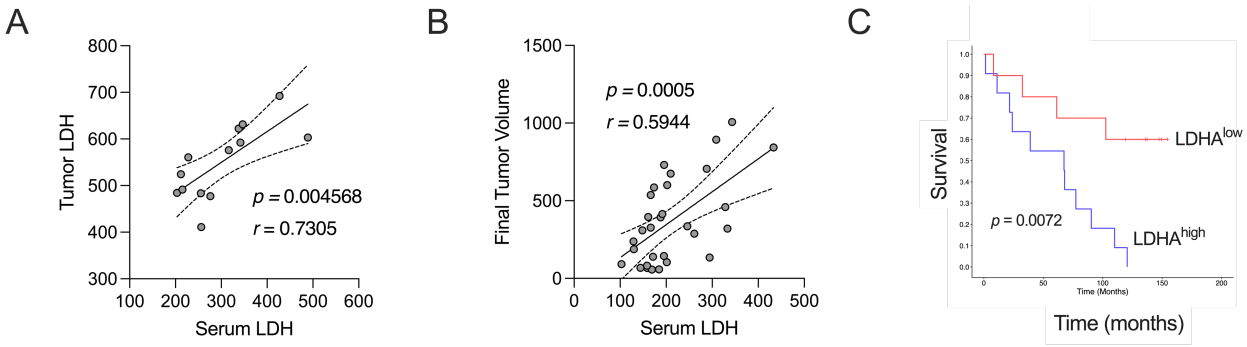

Supplemental Figure 2. LDH correlates with poor prognosis. (**A-B**) Correlations between B16 melanoma tumor LDH activity and serum LDH activity and between final B16 tumor burden and serum LDH activity quantified ex vivo from matched C57BL/6 mice 10 (**A**) and 20 (**B**) days of after tumor implantation, respectively. Data shown is representative of 3 independent experiments. Statistics produced by Spearman correlation tests in GraphPad. (**C**) Overall survival of melanoma patients stratified by tumor LDHA RNA expression. Samples were defined as LDHAhigh or LDHAlow by expression of LDHA above or below the median LDHA value across all samples respectively (Source: Riaz et al. (57)). Statistics produced by unpaired T test with Welch's correction implemented in R.

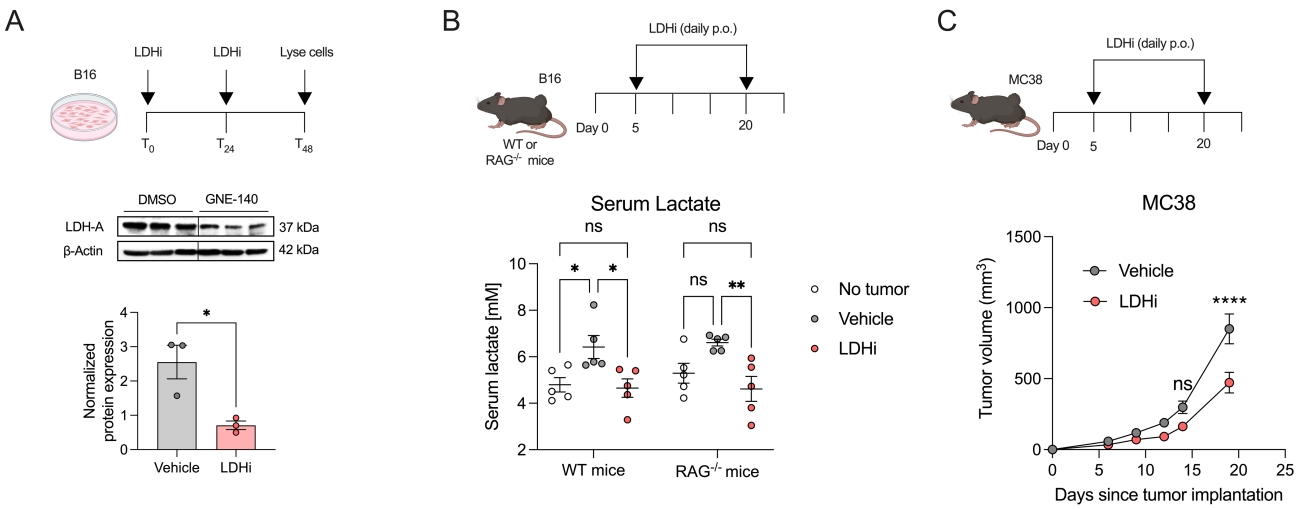

Supplemental Figure 3. Effects of LDHi in mouse tumor models. Corresponding to Main Figure 2. (**A**) Representative and densitometry quantification of western blot of LDHA and b-actin in whole cell lysates from B16 cells treated for 48hrs with 10 μM LDHi or vehicle control (DMSO). (**B**) Quantified serum lactate from the indicated B16-bearing mouse strains 1h after the last treatment with LDHi (100mg/kg) or control vehicle as indicated in the schema. (**C**) MC38 tumor growth curves upon treatment with LDHi (100 mg/kg) or control vehicle as indicated in the schema (n = 5/group). Data shown are one representative experiment of 3 independent experiments. All statistics produced by (**A**) Wilcoxon Rank Sum Test or (**B-C**) Two-way ANOVA with Bonferroni's multiple comparisons test implemented in GraphPad Prism in which *, $P<0.05$; **, $P<0.01$; ***, $P<0.001$; ****, $P<0.0001$. Data are mean +/– SEM.

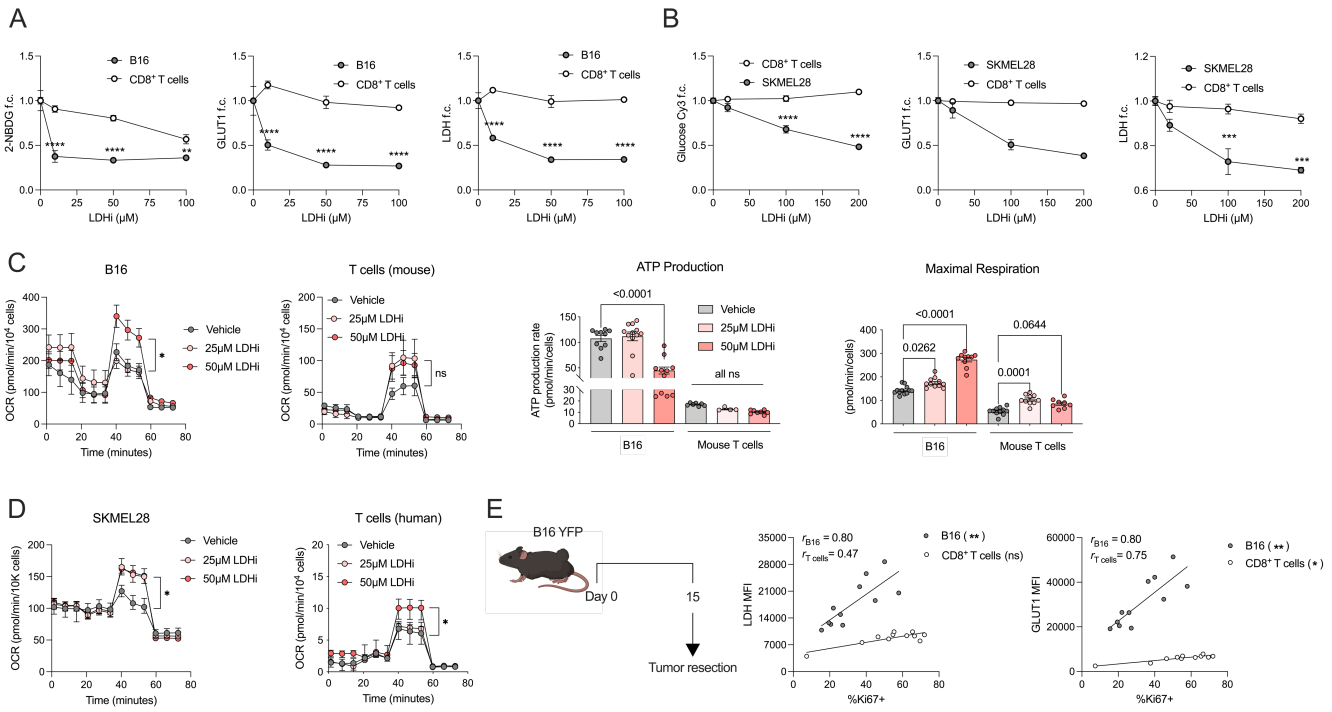

Supplemental Figure 4. Tumor cells display more glycolytic sensitivity to LDH inhibition than immune cells. Corresponding to Main Figure 3. (**A-B**) Fold-change values corresponding to data in Figure 3A-C, F-H. (**C**) Oxygen consumption rates (OCR), ATP production, and maximal respiration of B16 cells and activated mouse CD8$^+$ T cells treated with the indicated concentrations of LDHi or vehicle *in vitro,* normalized by cell number. Mouse T cells were treated with LDHi 24h post-aCD3/aCD28 activation and analyzed 24h later. (**D**) Oxygen consumption rates of SK-MEL-28 cells and activated human CD8$^+$ T cells treated with the indicated concentrations of LDHi or vehicle *in vitro*, normalized by cell number. Human T cells were treated with LDHi 48h post-aCD3/aCD28 activation and analyzed 24h later. (**E**) Correlations between LDH or GLUT1 expression (MFI) and %Ki67+ cells (gated based on the isotype control staining) in CD8$^+$ T cells and B16 YFP$^+$ tumor cells quantified by flow cytometry from B16 tumors from untreated mice. Data shown are one representative experiment of 3 independent experiments. All statistics produced by (**A-B**) Wilcoxon Rank Sum Test, (**E**) Pearson Correlation, and (**C-D**) Two-way ANOVA with Bonferroni's multiple comparisons test implemented in GraphPad Prism in which *, P<0.05; **, P<0.01; ***, P<0.001; ****, P<0.0001. Data are mean +/– SEM.

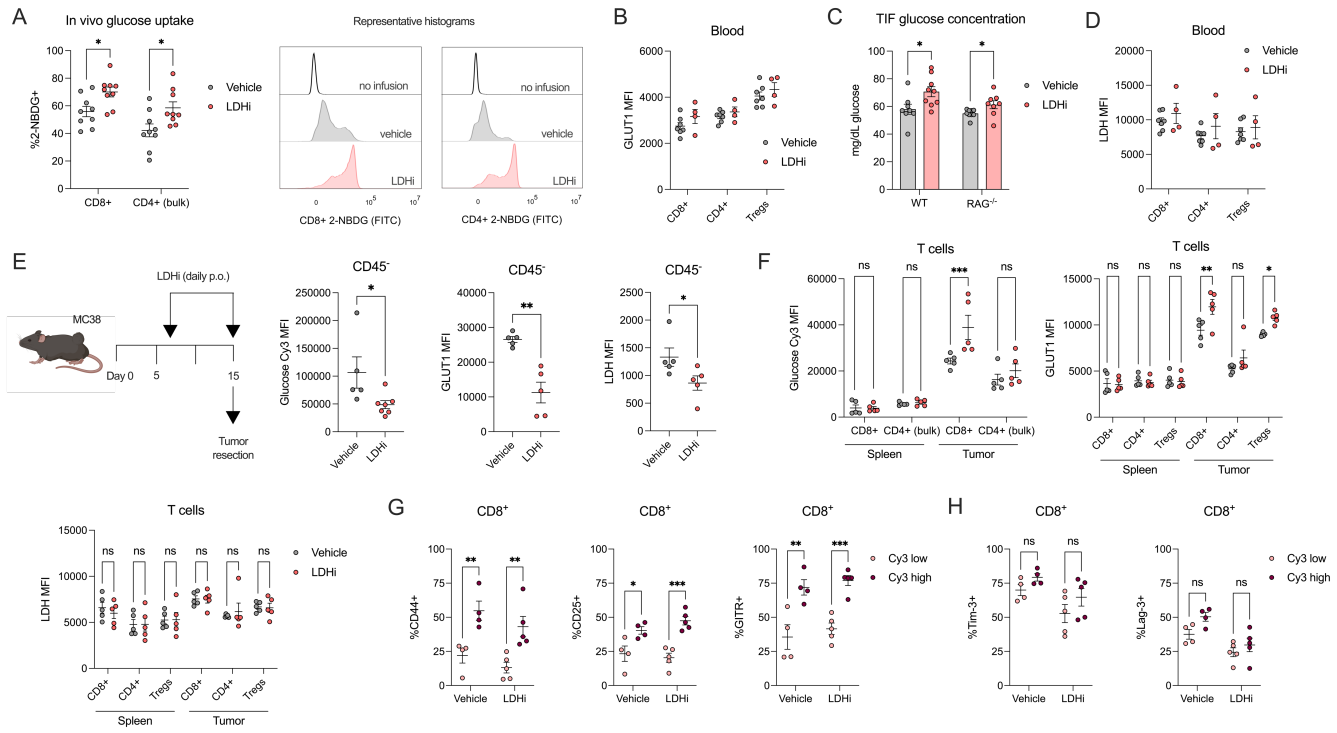

Supplemental Figure 5. LDHi boosts glucose uptake of intratumoral T cells with no bioactivity in blood cells. Corresponding to Main Figure 4. **(A-D)** Wild-type B16-bearing mice were treated with LDHi (100 mg/kg) or vehicle control for 10 days (n = 10/group) and (**A**) % 2-NBDG+ tumor-infiltrating T cells; and **(B)** GLUT1 and (D) LDH MFI in T cells from whole blood were quantified by flow cytometry; (**C**) and glucose concentrations in tumor interstitial fluid were quantified by glucose meter. **(E-F)** Quantification of Glucose Cy3, GLUT1, and LDH MFI by flow cytometry in (E) $CD45^-$ cells and **(F)** $CD8^+$, $CD4^+Foxp3^-$, and $CD4^+Foxp3^+$ T cell subsets isolated from tumors or spleens from MC38 bearing mice treated with LDHi (100 mg/kg) or vehicle control as indicated in the schema (n = 5 biological replicates). **(G-H)** Quantified (**G**) markers of activation: %CD44+, %CD25+, %GITR+, and (**H**) markers of exhaustion: %Tim3+, and %Lag3+, on B16 tumor-infiltrating CD8+ T cells stratified by high or low Glucose Cy3 uptake. Data shown are one representative experiment of 1-3 independent experiments. All statistics produced by Wilcoxon Rank Sum Test implemented in GraphPad Prism in which *, $P<0.05$; **, $P<0.01$; ***, $P<0.001$; ****, $P<0.0001$. Data are mean +/– SEM.

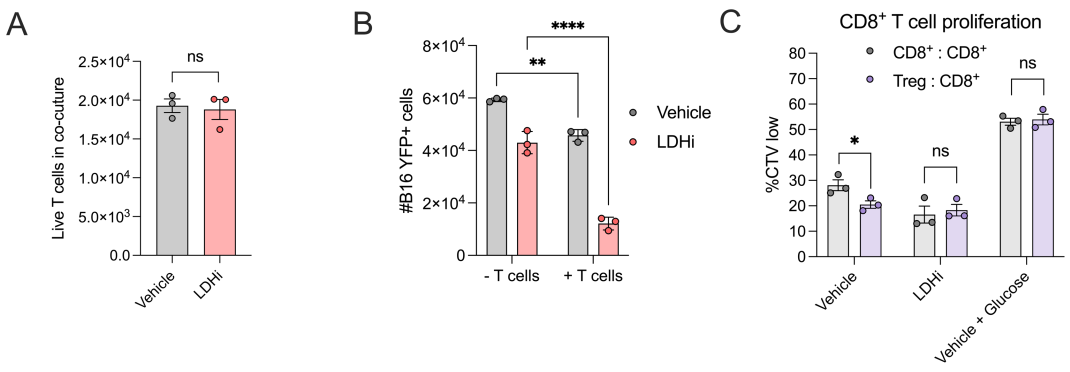

Supplemental Figure 6. LDH inhibition improves anti-tumor T cell functions. Corresponding to Main Figure 5. (**A**) Quantification of live $CD8^+$ T cells by flow cytometry after 48h killing assay co-culture, corresponding to experiment from Main Figure 5, C and D. (**B**) Raw data from Main Figure 5G: Quantification of live B16-YFP tumor cells from killing assay with $OVA_{257-264}$-pulsed live B16-YFP tumor cells and OVA-primed $CD8^+$ T cells from OT1 transgenic mice upon 48-hr co- culture in the presence of LDHi (as indicated in the schema from Main Figure 5A). Effector to target ratio, E:T = 2:1, co-cultured over 48h. (**C**) Raw data from Main Figure 5I: Quantification of $CD8^+$ T cell proliferation by CTV from in vitro Treg suppression assay with MACS column-sorted Tregs ($CD4^+CD25^+$ Regulatory T Cell Isolation Kit, mouse) co-cultured for 72hr with αCD3/αCD28 activated CTV-labeled syngeneic $CD8^+$ T cells and for 48hrs with the addition of conditioned media from B16 cells treated with 20 μM LDHi or vehicle, or fresh media containing 10 mM glucose. Data are from one representative experiment of 2-4 independent experiments (n = 3-4 biological replicates). All statistics produced by (**A**) Wilcoxon Rank Sum Test, and (**B-C**) Two-way ANOVA with Bonferroni's multiple comparisons test implemented in GraphPad Prism in which *, $P<0.05$; **, $P<0.01$; ***, $P<0.001$; ****, $P<0.0001$. Data are mean +/– SEM.

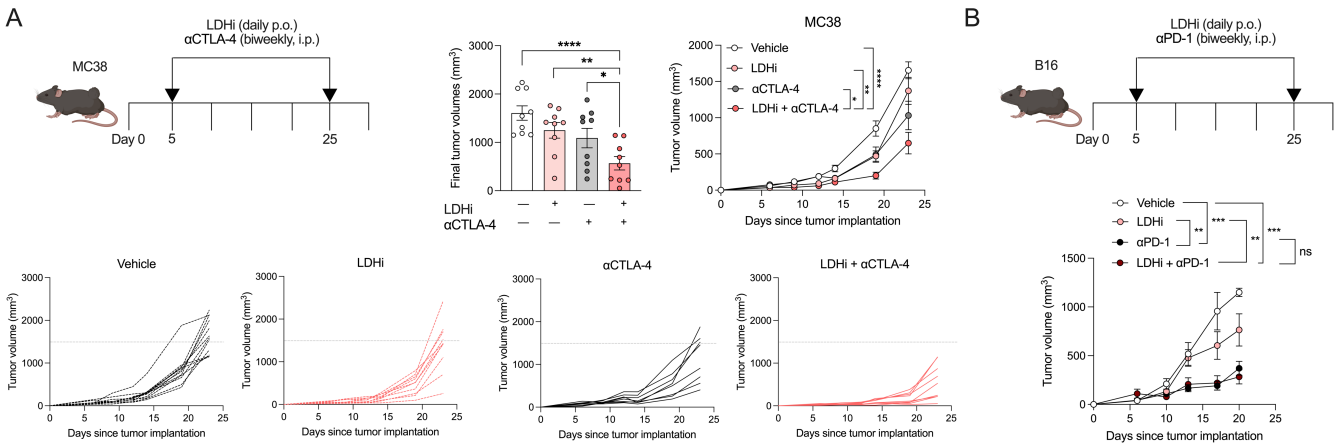

Supplemental Figure 7. Anti-tumor activity of LDHi with ICB in vivo. Corresponding to Main Figure 6. (**A**) Final tumor volumes and averaged and individual tumor growth curves (mm^3) from MC38 tumor-bearing mice treated with 100 mg/kg LDHi and/or CTLA-4 blockade (9D9, IgG2b) or control vehicle/IgG as indicated in the schema (n = 8-10 mice/group). (**B**) Tumor volumes (mm^3) from B16 tumor-bearing mice treated with early (day 5) PD-1 blockade (RPM1-14, IgG2b) and/or 100 mg/kg LDHi or control vehicle/IgG as indicated in the schema (n = 10-15 mice/group). Data are from one representative experiment of 2 independent experiments. All statistics produced by Wilcoxon Rank Sum Test or 2-way ANOVA implemented in GraphPad Prism in which *, $P<0.05$; **, $P<0.01$; ***, $P<0.001$; ****, $P<0.0001$. Data are mean +/– SEM.

Table S1. Flow cytometry antibody details.

Antibodies	Vendor	Cat No.	Clone
Zombie NIR	eBioscience	423105	N/A
BUV395 Rat Anti-Mouse CD45	BD Biosciences	564279	30-F11
BUV563 Rat Anti-Mouse CD62L	BD Biosciences	741230	MEL-14
BUV615 Rat Anti-Mouse CD8a	BD Biosciences	613004	53-6.7
BUV737 Hamster Anti-Mouse CD11c	BD Biosciences	612796	HL3
BUV805 Hamster Anti-Mouse TCR β Chain	BD Biosciences	748405	H57-597
Brilliant Violet 421 anti-T-bet	BioLegend	644816	4B10
Pacific Blue anti-mouse H-2Kb	BioLegend	116514	AF6-88.5
Pacific Blue anti-mouse H-2Kd	BioLegend	116616	SF1-1.1
BV480 Rat Anti-Mouse CD274 (PD-L1)	BD Biosciences	746275	MIH5
Brilliant Violet 510 anti-mouse/human CD11b	BioLegend	101263	M1/70
Pacific Orange anti-mouse F4/80	Invitrogen	MF48030	BM8
Brilliant Violet 570 anti-mouse Ly-6C	BioLegend	128029	HK1.4
Super Bright 645 anti-mouse CD19	Invitrogen	64-0193-82	eBio1D3 (1D3)
Super Bright 702 anti-mouse CD86 (B7-2)	Invitrogen	67-0862-82	GL1
BV750 Rat Anti-Mouse CD357 (GITR)	BD Biosciences	747402	DTA-1
Brilliant Violet 785 anti-mouse CD279 (PD-1)	BioLegend	135225	29F.1A12
Alexa Fluor 488 anti-mouse CD80	BioLegend	104716	16-10A1
Spark Blue 550 anti-mouse I-A/I-E	BioLegend	107662	M5/114.15.2
PerCP anti-mouse Ly-6G	BioLegend	127654	1A8
PerCP/Cyanine5.5 anti-mouse CD206 (MMR)	BioLegend	141715	C068C2
PerCP-eFluor 710 anti-mouse FOXP3	Invitrogen	46-5773-82	FJK-16s
PE/Dazzle 594 anti-mouse CD134 (OX-40)	BioLegend	119418	OX-86
PE-Cyanine5 anti-mouse EOMES	Invitrogen	15-4875-82	Dan11mag
PE-Cyanine7 anti-mouse CD152 (CTLA-4)	Invitrogen	25-1522-82	UC10-4B9
APC anti-mouse/human Granzyme B	Invitrogen	GRB05	GB11
Spark NIR 685 anti-mouse CD25	BioLegend	102070	PC61.5
Alexa Fluor 700 anti-mouse CD44	Invitrogen	56-0441-82	IM7
APC-eFluor 780 anti-mouse Ki-67	Invitrogen	47-5698-82	SolA15

APC/Fire 810 anti-mouse CD4	BioLegend	100480	GK1.5
BUV661 Hamster Anti-Mouse CD154 (CD40L)	BD Biosciences	741499	MR1
BUV496 Anti-Mouse H-2Ld/H-2Db	BD Biosciences	749923	28-14-8
Alexa Fluor 647 anti-glucose transporter (GLUT1)	Abcam	Ab195020	EPR3915
PE anti-lactate dehydrogenase (LDH)	Abcam	Ab210445	EP1563Y